CHEMICAL ENGINEERING TRANSACTIONS

VOL. 91, 2022

A publication of
AIDIC
The Italian Association
of Chemical Engineering
Online at www.cetjournal.it

Guest Editors: Valerio Cozzani, Bruno Fabiano, Genserik Reniers

**ISBN** 978-88-95608-89-1; **ISSN** 2283-9216

DOI: 10.3303/CET2291055

# Design and Optimization of an Emergency Auto-thermal Burner for Liquid Hydrogen

Alessandro Campari[a,b], Gianmaria Pio[b], Federico Ustolin[a], Nicola Paltrinieri[a], Ernesto Salzano[b,*]

[a] Department of Mechanical and Industrial Engineering, NTNU, Trondheim, Norway
[b] Dipartimento di Ingegneria Civile, Chimica, Ambientale e dei Materiali, Università di Bologna, Bologna, Italy
ernesto.salzano@unibo.it

The adoption of hydrogen has been largely indicated as a feasible solution to support society in achieving its ambitious targets for a low-carbon future. The increased knowledge in liquefaction techniques has encouraged the study of technological solutions based on liquid hydrogen ($LH_2$). Moreover, handling and distribution under cryogenic conditions represent attractive options due to the elevated energy density of $LH_2$. Despite these advantages, the bottleneck for its widespread adoption is represented by safety aspects. Considering that an $LH_2$ tank truck has a probability of suffering a car accident like all other road vehicles, an emergency auto-thermal burner has been designed in this work. This safety system has the purpose to dispose of the content of a tank truck to avoid the loss of containment. The disposal process includes the vaporization and pre-heating of the $LH_2$, the mixing with ambient air, and its combustion. This device is completely self-supporting since the heat required to vaporize the $LH_2$ is entirely provided by the combustion of the fuel itself. Firstly, the equation of energy balance around the burner was numerically solved to estimate the temperature of flue gases. Then, inner and outer heat transfer coefficients were determined for each section of the coiled-tube heat exchanger. Finally, the heat transfer surface was calculated. The spontaneous conversion between two spin isomers of hydrogen was considered. From the perspective of the heating process, the enthalpy of conversion represents an additional energy request. If the decrease of para-hydrogen fraction was neglected, the length of the heat exchanger would be significantly underestimated. Based on the obtained results, it is possible to conclude that the designed device can be transported on-site and started up easily, making it suitable for emergency response.

## 1. Introduction

The rising demand for clean and sustainable energy sources all over the world is stimulating research about alternative fuels for power generation, aviation, and road transport. The adoption of hydrogen has been largely indicated as a possible solution for social and environmental issues (IEA, 2019). The simultaneously increased knowledge in cryogenic liquefaction techniques and the development of proper large-scale tanks have recently encouraged the study of technological solutions based on liquid hydrogen (Valenti, 2016). The main advantage of storing by liquefaction is the density of $LH_2$, which is around 70.9 kg/m$^3$. On a mass basis, hydrogen shows the highest LHV, equal to 119.93 MJ/kg. In contrast, liquid hydrogen is characterized by a relatively low heating value on a volume basis, i.e., 8.49 GJ/m$^3$ (NIST, 2021). Cryogenic liquid fuels can be stored and transported in double-walled vessels. The purpose of these special containers is to protect the cryogen from the conductive, convective, and radiative heat transfer from the outside. An efficient insulation system is crucial for storing and transporting $LH_2$ since makes it possible to minimize the boil-off. Vacuum-insulated vessels are the great majority of containers for cryogenic fuels. In particular, multi-layer insulation (MLI) is used for its extremely low thermal conductivity, radiation heat transfer, and density (Valenti, 2016). On the other hand, in case of loss of vacuum, a near-catastrophic failure of the containment system may occur (Molkov, 2012). Super-insulated tanker trucks have a capacity ranging from 20 to 50 m$^3$ and can store up to 4,000 kg of $LH_2$ at a pressure that usually ranges from 6 to 10 bar (Usolin *et al.*, 2019). These trucks are commonly used for journeys of up to

Paper Received: 9 January 2022; Revised: 30 March 2022; Accepted: 4 May 2022
Please cite this article as: Campari A., Pio G., Ustolin F., Paltrinieri N., Salzano E., 2022, Design and Optimization of an Emergency Auto-thermal Burner for Liquid Hydrogen, Chemical Engineering Transactions, 91, 325-330 DOI:10.3303/CET2291055

4,000 km, but they are not suitable for transport above this distance as the hydrogen heats up and the pressure inside the tank tends to rise considerably (Decker, 2016). Accidental leaks of liquid hydrogen might occur after severe car accidents. Holes and fractures in the containment system may release large amounts of cryogenic fuel in the environment, that rapidly vaporizes, mixes with air, and forms a flammable mixture. Several categories of fire and explosion events, such as jet fires, pool fires, flash fires, vapor cloud explosions (VCE), and boiling liquid expanding vapor explosion (BLEVE), may occur in presence of ignition sources (Ustolin *et al.*, 2019). Moreover, a loss of integrity of the super-insulated vessel may expose personnel to direct contact with an ultra-low temperature fluid. Besides the extreme temperature, the $LH_2$ has low viscosity, which enables it to penetrate through porous material very quickly. If $LH_2$ gets in direct contact with the human skin, can cause severe damages and potentially lethal injuries (Molkov, 2012). Considering that an $LH_2$ tank truck has a probability of suffering a car accident comparable with that of all other road vehicles, it is of the utmost importance to design safety devices able to guarantee an acceptable level of security during transport. The emergency auto-thermal burner designed in this work has the purpose to dispose of the content of a large-size tank truck in case of accidents that may lead to failure of the containment system and accidental release of $LH_2$ in the environment.

## 2. Emergency auto-thermal burner

The emergency system is mainly composed of three coiled-tube heat exchangers: the economizer, the vaporizer, and the superheater. The chemical reactor upstream of the superheater represents the transition (i.e., the para-ortho conversion) taking place within the pipe. The proper amount of air is fed to the premix burner by a fan. The by-pass line allows overriding the economizer if there is no liquid phase left within the tank. After a car accident, if the containment system does not show leaks or fractures, the emergency burner should be connected to the vessel through a flange. The liquid hydrogen spilled from the vessel passes through the economizer, the vaporizer, and the superheater; all these heat exchangers are tube-shaped and directly flame heated. When the $LH_2$ has turned to gaseous hydrogen, its temperature rises sharply, then its chemical composition tends to correspondingly change (due to the para-to-ortho conversion); in particular, the ortho-para ratio rises with increasing temperature (Milenko *et al.*, 1997). It is noteworthy that this emergency device is completely self-supporting. The heat required to vaporize the $LH_2$ is entirely provided by the combustion of the fuel itself. A simplified process flow diagram of this safety device is represented in Figure 1 below.

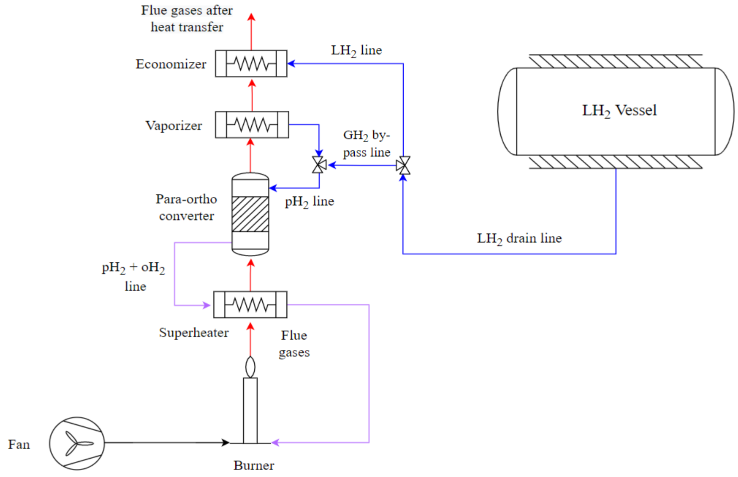

*Figure 1: Process flow diagram of the emergency burner for liquid hydrogen*

## 3. Methodology

Information about the equivalence ratio of the flammable mixture, the temperature of exhaust gases, the heat transfer coefficients, and the para-to-ortho conversion are provided in the following subsections.

### 3.1 Assumptions

The technical characteristics of the super-insulated truck trailer have been hypothesized based on the projects of the major companies which operate in the field of cryo-liquefied gases (Decker, 2016). The volume of the vessel is the maximum currently being used for road transport of liquefied gases. The main technical specifications of the $LH_2$ tank truck are summarized in Table 1.

*Table 1: Technical specifications of the $LH_2$ truck trailer (Decker, 2016)*

| | Symbols | Set values |
|---|---|---|
| Volume of the vessel ($m^3$) | $V_{tank}$ | 50 |
| Operating pressure (bar) | $p_{LH_2}$ | 8 |
| Operating temperature (°C) | $T_{LH_2}$ | -253 |
| Mass of $LH_2$ (kg/s) | $m_{LH_2}$ | 3,51 |
| Maximum time for discharge (h) | $t_{max}$ | 3 |

Hydrogen has a laminar burning velocity one order of magnitude higher than conventional fuels' one (Pio and Salzano, 2018). To minimize the flame instability, it is important to lower the burning velocity of hydrogen. Since the purpose of the emergency burner is to dispose of the largest amount of fuel in the shortest possible time, a feasible solution is to burn a very rich air-fuel mixture. If the equivalence ratio of a hydrogen-air mixture ranges from 7 to 8, the burning velocity is of the same order of magnitude as that of a methane-air stoichiometric mixture. In fact, at 0 °C a hydrogen-air mixture with an equivalence ratio of 7, and a methane-air mixture with an equivalence ratio of 1.1 have laminar burning velocities equal to 50 cm/s and 35.5 cm/s, respectively (Pio and Salzano, 2018).

### 3.2 Design of the burner

Considering a rich hydrogen-air mixture ($\varphi$ = 7), the major components of flue gases are nitrogen, hydrogen, and water. The energy balance around the burner has the following expression:

$$\varepsilon\,\dot{m}_{H_2} LHV - \dot{Q}_{rad} - \dot{m}_g \int_{T_0}^{T_g} c_{p\,g}(T)\,dT + \dot{m}_{H_2} \int_{T_0}^{T_{H2}} c_{p\,H_2}(T)\,dT + \dot{m}_a \int_{T_0}^{T_a} c_{p\,a}(T)\;dT = 0 \tag{1}$$

where $\varepsilon$ is the combustion efficiency, $\dot{m}$ the mass flow (kg/s), $LHV$ the lower heating value (kJ/kg), $\dot{Q}_{rad}$ the radiative losses (kW), $c_p$ the heat capacity (kJ/kg K); subscript $H_2$ represents hydrogen, $g$ the exhaust gases, and $a$ the ambient air. The heat capacity of a gas can be expressed through a polynomial function of the temperature (Perry *et al.*, 1997). The numerical coefficients are supplied in the Reaction Mechanism Generator (RMG) database (Green and West, 2021). Given the coefficients for each chemical species, the polynomial function can be easily integrated. The unknown exhaust gases temperature $T_g$ is calculated through Newton-Raphson's algorithm in MATLAB. Since the energy required to preheat the liquid hydrogen, vaporize it, and superheat the $GH_2$ is entirely provided by the enthalpy of combustion of the fuel itself, the flue gases are cooled by the hydrogen which flows into the tube. The heat exchanged is given by Eq. 2:

$$\dot{m}_{H_2}\left[\int_{T_{LH2}}^{T_{H2\,eva}} c_{LH_2}(T)\,dT + \Delta H_{eva\,H_2}(T,p) + \int_{T_{H2\,eva}}^{T_{H2}} c_{p\,H_2}(T)\,dT\right] = -\dot{m}_g \int_{T_g}^{T_{g\,2}} c_{p\,g}(T)\,dT \tag{2}$$

where $\Delta H_{eva}$ is the latent heat of vaporization (kJ/kg); $T_{LH2}$ and $T_{H2\,eva}$ are the storage temperatures of liquid hydrogen and its boiling point (°C), respectively; $T_g$ and $T_{g\,2}$ are the temperatures of exhaust gases before and after heat transfer (°C), respectively. Exhaust gases move vertically thanks to the natural draft; they transfer heat to the hydrogen, which flows within the coiled tube. The total heat transferred is given by three additive terms: the thermal powers exchanged within the economizer, the vaporizer, and the superheater.

*Table 2: Transferred thermal power within each section of coiled-tube heat exchanger*

| Heat exchanger | Transferred thermal power | |
|---|---|---|
| Economizer | $\dot{Q}_{eco} = U_{eco}\,A_{eco}\left(T_g - T_{LH_2}\right) = \dot{m}_{H_2}\int_{T_{LH2}}^{T_{H2\,eva}} c_{LH_2}(T)\,dT$ | (3) |
| Vaporizer | $\dot{Q}_{vap} = U_{vap}\,A_{vap}\left(T_g - T_{H_2\,eva}\right) = \dot{m}_{H_2}\,\Delta H_{eva\,H_2}(T,p)$ | (4) |
| Superheater | $\dot{Q}_{ssh} = U_{ssh}\,A_{ssh}\left(T_g - T_{H_2}\right) = \dot{m}_{H_2}\int_{T_{H2\,eva}}^{T_{H2}} c_{p\,H_2}(T)\,dT$ | (5) |

where $\dot{Q}$ is the thermal power transferred (kW), $U$ is the overall heat transfer coefficient (kW/$m^2$ K) and $A$ is the heat transfer surface ($m^2$). Both the heat transfer surface and the overall heat transfer coefficient are unknown. Then, inner and outer heat transfer coefficients should be determined for each heat exchanger, depending on the flow regime within the pipe.

Since the exhaust gases are a mixture, the thermophysical properties are calculated as a weighted average of the properties of pure compounds. The coil can be considered a circular duct with high roughness in which exhaust gases flow in a turbulent regime. The outer heat transfer coefficient is calculated through the correlation developed by Martinelli (1947), while the Darcy friction factor is determined by the correlation proposed by Von Kármán (1939):

$$h_{ext} = \frac{Re\ Pr\ [(3.36 - 1.767\ \ln(\varepsilon/D_{coil}))^{-2}/2]^{0.5}}{5\left\{Pr + \ln(1 + 5\ Pr) + 0.5\ \ln\frac{Re\ [(3.36 - 1.767\ \ln(\varepsilon/D_{coil}))^{-2}/2]^{0.5}}{60}\right\}} \cdot \frac{k_g}{D_{coil}} \tag{6}$$

where $Re$ and $Pr$ are Reynolds and Prandtl numbers, respectively, $\varepsilon$ is the roughness of the duct (µm), $D_{coil}$ the coil diameter (m), and $k_g$ the thermal conductivity of exhaust gases (W/m K).

Liquid hydrogen flowing along the economizer is a sub-cooled liquid. The heat transfer coefficient for a fully developed turbulent flow within the pipe can be estimated by the following correlation for heating (Dittus and Boelter, 1985):

$$h_{eco} = 0.023\ Re^{0.8} Pr^{0.4} \cdot \frac{k_{LH_2}}{D} \tag{7}$$

where $D$ is the pipe diameter (m) and $k_{LH_2}$ the thermal conductivity of liquid hydrogen (W/m K).

The hydrogen enters the vaporizer as a saturated liquid. Assuming that the convective and nucleate boiling contributions are additive, the following correlation (Chen, 1966) can be used to determine the heat transfer coefficient:

$$h_{vap} = \frac{1}{1 + 2.53 \cdot 10^{-6} [Re_L\ 2.35\ (X_{tt}^{-1} + 0.213)^{0.736}]^{1.17}} \cdot h_{nb} + 2.35\ (X_{tt}^{-1} + 0.213)^{0.736} \cdot h_{eco} \tag{8}$$

where $Re_L$ is the Reynolds number for liquid-phase only, $X_{tt}$ the Lockhart-Martinelli parameter, and $h_{nb}$ the nucleate boiling heat transfer coefficient W/m$^2$ K), calculated through the correlation proposed by Forster and Zuber (1955).

The sharp increase in hydrogen temperature taking place within the superheater leads to a variation of its thermophysical properties. In addition, it is important to consider the variable concentration of para- and ortho-hydrogen along the tube. All the thermophysical properties can be determined as an average of the properties of the pure fluids, weighted on the ortho-hydrogen fraction. The heat transfer coefficient is calculated by the correlation proposed by Gnielinsky (1976), while the friction factor is calculated by the Colebrook one (Brkić, 2011):

$$h_{ssh} = \frac{[(0.782\ \ln(Re) - 1.51)^{-2}/8]\ (Re - 1000)\ Pr}{1 + 12.7\ \sqrt{(0.782\ \ln(Re) - 1.51)^{-2}/8}\ (Pr^{2/3} - 1)} \cdot \frac{k_{H_2}}{D} \tag{9}$$

The equilibrium concentration of para- and ortho-hydrogen is a function of the temperature: at the liquefaction temperature, almost all the hydrogen is in para-form, while at the ambient temperature it shows a 3:1 ortho-to-para ratio. Therefore, a spontaneous para-ortho conversion occurs along the pipe. From the perspective of the heating process, the enthalpy of conversion of this endothermic reaction is an additional heating load. The conversion rate is calculated through a second-order rate equation (Milenko *et al*., 1997):

$$\frac{dc_{oH_2}}{dt} = k_{p\to o} \cdot c_{oH_2} \cdot (1 - c_{oH_2}) - k_{o\to p} \cdot c_{oH_2}^2 \tag{10}$$

where $k_{p\to o}$ and $k_{o\to p}$ are the conversion constants of the direct and reverse reaction, respectively, and $c_{oH_2}$ is the concentration of ortho-hydrogen.

The conversion constant of the ortho-para transformation is given by (Milenko *et al*., 1997):

$$k_{o\to p} = (18.2 + 1.6) \cdot T^{0.56\pm0.02} \cdot \rho + 5 \cdot 10^4 \cdot [0.77 + 0.03 + (921 + 91) \cdot T^{-2.5\pm0.2}] \cdot \rho^{3.6} \tag{11}$$

where $T$ is the hydrogen temperature (K) and $\rho$ is the density (g/cm$^3$).

The difference in hydrogen internal energy between the inlet and outlet of the pipe shall be equal to the heat transferred from exhaust gases to the cryogenic fuel. The heat transfer surface is unknown. Setting the diameter of the pipe, the length is calculated through the following differential equation:

$$\frac{d\ l_{pipe}}{d\ T} = \frac{2}{\pi\ D} \cdot \frac{\dot{m}_{H_2} c_{p\ H_2}(T)}{U(T)} \cdot \frac{1}{T_g - T} \tag{12}$$

This equation can be used for the stretches of pipe where sensible heat is transferred. However, hydrogen does not vary its temperature into the vaporizer but gradually increases the vapor fraction. Hence, Eq. 13 can be integrated with respect to the variable $x$, i.e., the vapor fraction ($kg_{vap}/kg$):

$$\frac{d\, l_{pipe}}{d\, x} = \frac{2}{\pi\, D} \cdot \frac{\dot{m}_{H_2} \Delta H_{eva\, H_2}}{U(x)} \cdot \frac{1}{T_g - T_{H_2\, eva}} \tag{13}$$

The equations above were solved through the Runge-Kutta fourth-order method.

## 4. Results and discussion

Temperatures of combustion products before and after heat transfer with cryogenic hydrogen are represented as functions of equivalence ratio in Figure 2.

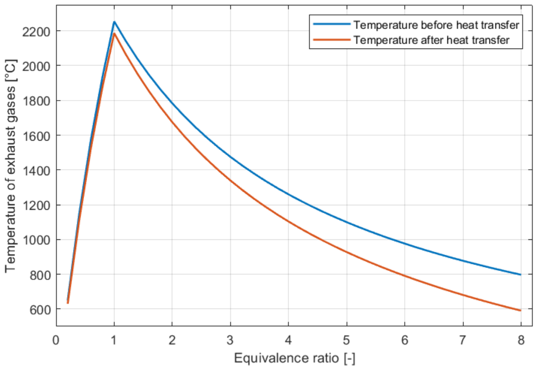

*Figure 2: Temperature of exhaust gases before and after heat transfer as functions of equivalence ratio*

For a stoichiometric mixture, the calculated adiabatic flame temperature is 2254 °C; this result matches with experimental data for the combustion of hydrogen in air (Molkov, 2012). The decrease in temperature of flue gases after heat transfer with hydrogen becomes more significant for the higher equivalence ratios. In fact, the greater $\varphi$ is, the greater becomes the flow rate of hydrogen that must be heated up to near-ambient temperature. Radiative losses tend to reduce the temperature of exhaust gases, consequently increasing the total length of the pipe. In Figure 3 (a) the heat transfer coefficient within the vaporizer is represented as a function of the vapor fraction, while Figure 3 (b) shows the heat transfer coefficient into the superheater as a function of temperature.

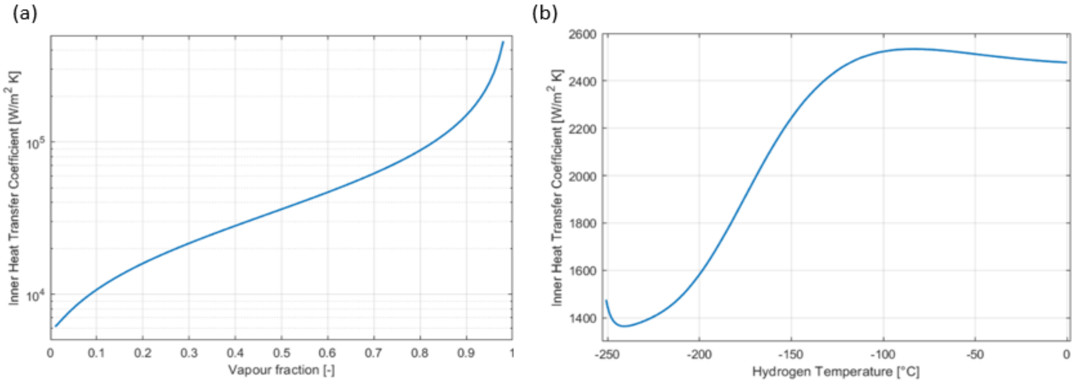

*Figure 3: Inner heat transfer coefficients within the vaporizer (a) and the superheater (b)*

At the evaporation temperature, the boiling regime onsets within the vaporizer, and the heat transfer coefficient rises sharply. As the vapor fraction increases, the heat transferred tends to enhance gradually and then falls abruptly when the boiling regime ends. During the vaporization, the temperature difference between the pipe wall and the boiling hydrogen remains almost constant (approximately 6.5 °C); the resulting wall temperature is ultra-low since the inner heat transfer coefficient is dramatically greater than the outer. The gaseous hydrogen temperature varies from −250.9 °C to 0 °C through the superheater. All the thermophysical properties of the fluid vary sharply with temperature; moreover, its chemical composition is not constant since the fraction of ortho-hydrogen increases as the fuel approaches the outlet of the pipe. The minimum heat transfer coefficient can be observed for a temperature around −240 °C; within the range −240 ÷ −100 °C, it rises to 2530 $W/m^2$ K.

For temperatures higher than −100 °C, the heat transfer coefficient remains approximately constant, since the decreases in density, heat capacity, and dynamic viscosity are counterbalanced by the sharp increases in fluid speed and thermal conductivity. In equilibrium conditions, at 0 °C the fraction of ortho-hydrogen would be approximately 75 %. Nevertheless, a complete para-to-ortho conversion cannot occur because the residence time of hydrogen at high temperature is too short to reach the equilibrium. Eq. (7), solved through the Runge-Kutta method, shows that the maximum ortho-hydrogen fraction is slightly lower than 50 %. Setting the diameter of the coil and the pipe equal to 1 m and 3.8 cm, respectively, the characteristic dimensions of the emergency auto-thermal burner are summarized in Table 3:

*Table 3: Technical specifications of the emergency burner*

| | Symbols | Economizer | Vaporizer | Superheater |
|---|---|---|---|---|
| Mass flow rate (kg/s) | $\dot{m}_{H_2}$ | 0.1625 | 0.162 | 0.1625 |
| Operating pressure (bar) | $p$ | 1.75 | 1.74 | 1.70 |
| Temperature difference (°C) | $\Delta T$ | 4.1 | - | 250.9 |
| Pipe length (m) | $l_p$ | 0.85 | 13.2 | 104.5 |
| Coil height (cm) | $H_{coil}$ | 3.8 | 17.6 | 140 |

## 5. Conclusions

An emergency system capable of safely disposing of the $LH_2$ tank truck content was designed. This device is completely self-supporting, lightweight, and does not require any heat transfer fluid; it is specifically designed to avoid a near-catastrophic failure of the containment system in case of a car accident. Given the high flow rate of hydrogen to burn in a limited time, two burners can be connected in parallel to speed up the process. This allows using small-sized heat exchangers and fans, making also possible a modular control of the process. The spontaneous para-to-ortho conversion was considered. The results show that, if the decrease of para-hydrogen fraction was neglected, the length of the superheater's pipe would be underestimated by almost 5 m. The main disadvantage of this device is the difficulty to bypass the economizer and the vaporizer when remains gaseous fuel only within the tank; in the final stage of the discharge process, the emergency burner can operate in off-design conditions. It is possible to conclude that the designed device can be transported on-site and started up easily, making it suitable for emergency response in case $LH_2$ is involved.

### References

Brkić D., 2011, Review of explicit approximations to the Colebrook relation for flow friction, J.Pet.Sci., 77, 34-48

Chen J.C., 1966, Correlation for boiling heat transfer to saturated fluids in convective flow, Ind. Eng. Chem. Process. Des. Dev., 5, 322-329.

Decker L., 2016, Liquid Hydrogen Distribution Technology - HYPER Closing Seminar, Bruxelles, 11/10/2019.

Dittus W., Boelter L.M.K., 1985, Heat Transfer in Automobile Radiators of the Tubular Type, Int. Commun. Heat Mass Transf., 12, 3-22.

Forster H.K., Zuber N., 1955, Dynamics of vapor bubbles and boiling heat transfer, AIChE Journal, 1, 531-535.

Gnielinsky V., 1976, New Equations for Heat and Mass Transfer in Turbulent Pipe and Channel Flow, Int. J. Chem. Eng., 16, 359-36.

Green W.H., West R.H., 2021, RMG Thermodynamics Libraries, accessed 27/10/2021.

International Energy Agency (IEA), 2019, The Future of Hydrogen: Seizing today's opportunities.

Martinelli R.C., 1947, Heat Transfer to Molten Metals, J. Fluids Eng., 69, 947-959.

Milenko Y.Y., Sibileva R.M., Strzhemechny M.A., 1997, Natural Ortho-Para Conversion Rate in Liquid and Gaseous Hydrogen, J. Low Temp. Phys., 107, 77-92.

Molkov V., 2012, Fundamentals of Hydrogen Safety Engineering I, Bookboon.

NIST, 2021, NIST Chemistry WebBook, accessed 27/10/2021.

Perry R.H., Green D.W., Maloney J.O., 1997, Perry's Chemical Engineers' Handbook - 7th Edition, Chemical Engineering Handbooks, McGraw-Hill.

Pio G., Salzano E., 2018, Laminar Burning Velocity of Methane, Hydrogen, and Their Mixtures at Extremely Low-Temperature Conditions, Energy Fuels, 32, 8830–8836.

Ustolin F., Song G., Paltrinieri N., 2019, The influence of H2 safety research on relevant risk assessment, Chem. Eng. Trans., 74, 1393–1398.

Valenti G., 2016, Hydrogen liquefaction and liquid hydrogen storage, Compendium of Hydrogen Energy: Volume 2 - 1st Edition, Woodhead Publishing.

Von KármánT., 1939, The Analogy Between Fluid Friction and Heat Transfer, 61, J. Fluids Eng., 705.